Journal of Materials Chemistry C

Accepted Manuscript

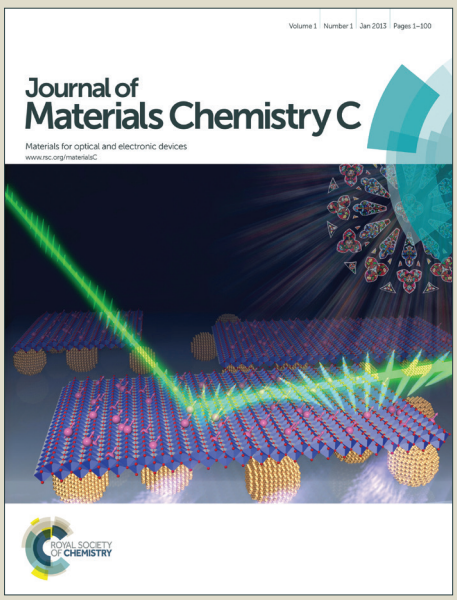

ROYAL SOCIETY OF CHEMISTRY

www.rsc.org/materialsC

Plasmonic Enhancement of Dual Mode Fluorescence in Silver Nano Antenna - ZnO:Er^{3+} Hybrid Nanostructure

*Rupali Das, Parikshit Phadke, Naveen Khichar and Santa Chawla**

Luminescent Materials Group, National Physical Laboratory, Dr.K.S.Krishnan Road, New Delhi-110012, India

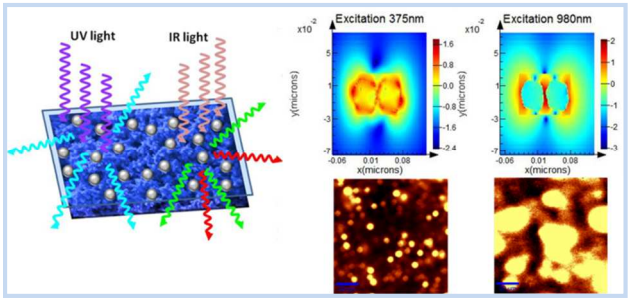

Plasmonic enhancement of dual mode fluorescence in Er^{3+} doped ZnO nanoparticles by shape tailored Ag nanoparticles

Journal Name

RSCPublishing

ARTICLE

Plasmonic Enhancement of Dual Mode Fluorescence in Silver Nano Antenna - ZnO:Er^{3+} Hybrid Nanostructure

Cite this: DOI: 10.1039/x0xx00000x

Received ooth January 2012,
Accepted ooth January 2012

DOI: 10.1039/x0xx00000x

www.rsc.org/

*Rupali Das, Parikshit Phadke, Naveen Khichar and Santa Chawla**

The ability to tune surface plasmon resonance (SPR) of silver nanoparticles (Ag NPs) through shape tailoring make them frequency tunable multipolar optical nano antennas that can be harnessed for optical enhancements in a fluorophore placed in optimal proximity. Such tuning of SPR has been achieved with Ag nanohexagon such that enhancement in both down (under UV excitation) and up (under IR excitation) conversion fluorescence from rare earth Er^{3+} doped ZnO nanoparticles is realized. The near field generated by exact Ag NPs and their hybrids under UV and IR incident light is simulated through Finite difference time domain method and a direct correlation with observed fluorescence enhancement is established.

Introduction

Shape tailored noble metal nanoparticles (MNPs) have the distinctive ability to confine and enhance incident electromagnetic (EM) field around them through coherent collective oscillation of surface electrons termed as surface Plasmon resonance (SPR) in distinct dipolar and multipolar modes[1] as well as lightening rod effect. MNPs e.g., silver nanoparticles (Ag NPs) can thus behave like multipolar optical nano antennas, SPR modes of which can be tuned through tailoring of shape, size and its dielectric environment. The near field of Ag NPs can couple to either excitation or emission frequencies of a fluorophore placed at a proximal distance leading to fluorescence enhancement[2] for which SPR of Ag NPs must overlap with either absorption or emission band of the fluorophore. Coupling of metal semiconductor hybrid nanostructures at optical frequencies for enhanced performance is of particular interest for applications such as solar cells, solid state lighting, biological imaging etc. For effectiveness of such coupled hybrid system, tailoring and matching properties of both the constituent components is extremely important. Direct band gap semiconductor like ZnO has a great advantage in this regard as it is an excellent emitter in the UV-visible region and can also accommodate discrete 4f levels of light emitting trivalent rare earth (RE) ions in its wide forbidden gap to tune the excitation and emission range. Despite importance of ZnO as tunable light emitter, report on ZnO-MNP hybrids for fluorescence enhancement are rare. [3-9] Designed EM field of shape and size tailored Ag NPs is shown to have significant role in fluorescence enhancement of RE ions[10-12]. In metal semiconductor hybrid nanostructures, surface plasmon modes and wave functions of bound excitons can remain unperturbed in the weak coupling region and the interaction of plasmon EM field with emitting dipole could lead to enhanced absorption when SPR matches with the absorption band of the semiconductor NP. Undoped ZnO has excitation in the UV (band edge excitation ~370 nm) and emission in the visible due to recombination of electron hole pairs in intrinsic defects. ZnO NPs can be made a upconversion (UC) luminescence emitter by doping with appropriate lanthanum ion like Erbium (Er^{3+}) which can absorb infra red (IR) light due to transition between its discrete 4f levels ($^4I_{15/2}$ - $^4I_{11/2}$). Hence Er^{3+} doping in ZnO NPs could make it dual absorber of both UV and IR EM field with visible, intrinsic emission under UV and characteristic green/red Er^{3+} UC luminescence under IR excitation. In order to achieve enhanced dual mode luminescence from such ZnO:Er^{3+} NPs in a metal semiconductor hybrid nanostructure, the SPR of metal (Ag NPs) has to be tuned to match both the excitation range in UV and IR. Photoluminescence (PL), however, is often quenched due to non radiative charge transfer processes between semiconductor and metal particles in direct contact. To enhance plasmon-bound exciton interactions, a dielectric spacer layer in the form of linker molecules must be introduced for effective separation and avoid luminescence quenching. To achieve this, we have used colloid chemistry to fabricate shape and size tailored Ag NPs for tuning SPR as well as to attach specific linker molecules to Ag NPs.

In the present work, we explore the multipolar character of silver nanohexagons and employ quadrupolar and dipolar SPR modes in UV and IR region to couple with specific excitation energy of RE ion (Er^{3+}) doped ZnO nanoparticles to achieve dual mode luminescence enhancement. The novelty of the work is in tuning surface Plasmon modes by shape tailoring silver nanoparticles and coupling such modes with fluorescent nanoparticles in both UV and IR spectral regions to harness optical enhancement in the visible region, which has immense importance from device point of view. Plasmon enhanced fluorescence from Er^{3+} has been reported for gold nanowire-$NaYF_4$:Yb,Er[13], Ag-SiO_2-Y_2O_3:Er nanostructure[14], gold nanosphere-$NaYF_4$:Yb,Er nanocrystals[15], Ag NP-Bismuth Germanate glasses[16]. To the best of our knowledge, no work has been reported on dual mode luminescence enhancement in doped ZnO–Ag NP hybrid structure or any other fluorophore. We report luminescence enhancement in both down and up conversion emission from Er^{3+} doped ZnO nanoparticles in proximity of SPR tuned Ag NPs. In order to comprehend the enhancement of fluorescence with mutipolar near field generated around Ag NPs, FDTD simulation has been carried out for representative Ag nanohexagon and their hybrids under UV and IR incident radiation and a cause – effect relationship is established.

Experimental

Trivalent rare earth Er^{3+} (2 atomic%) doped ZnO nanoparticles were synthesized by co-precipitation (CPP) method at room temperature using submolar precursor solutions of zinc acetate and erbium nitrate as CPP technique ensured effective incorporation of dopant in nano-sized ZnO. XRD confirmed monophasic wurtzite hexagonal ZnO structure [see supporting figure S1]. The morphological analysis revealed hierarchical flower like formation (Fig. 1a). The inset in Fig.1b shows the magnified TEM image of a single flower comprising individual nanoparticles (~5 nm) as revealed in the HRTEM image showing well formed lattice fringes (Fig.1b) [see supporting figure S2]. Ag NPs were synthesized by optimizing the method developed by Meutrax and Mirkin[17] to yield an Ag NP solution with blue colour, the colour being a consequence of its SPR band. The solution comprises mostly of polygonal Ag NPs like hexagon with edge length~50nm as evident from collage of TEM images (Fig.1c). Typical thickness of nanohexagons is about 25 nm, as measured from TEM micrographs. The ZnO:Er^{3+} and Ag NPs integrated hybrid nanostructure in a thin film configuration was prepared by controlled drop casting on a microscope cover slip. The material system was conjugated with first drop casting a thin layer of ZnO:Er^{3+} nanoparticles dispersed in PVA (3% PVA in water) on the substrate followed by a thin layer of Ag NPs. The PVA spacer layer averts formation of any silver oxide at the AgNP-ZnO:Er^{3+} interface due to oxidation and also prevents the quenching of fluorescence due to intervening non-radiative transitions when Ag NPs are placed in the proximity of the fluorescent NPs[18]. The deposition and conjugation parameters for dielectric spacer layer were optimized to realize metal enhanced fluorescence. The thickness of PVA spacer layer as measured by optical profilometry is about 100nm. A systematic study of PVA concentration and layer deposition parameters for metal enhanced fluorescence has been reported[11,12] and in most inorganic nanoparticles and Ag NP combination the spacer layer thickness as employed in the present case produce good results**.** The graphical representation of ZnO:Er^{3+} nanoflower–PVA layer-Ag NPs integrated thin film system used for confocal fluorescence microscopy is shown in Fig.1(d), to clearly elucidate the different components in the integrated material system. The light is incident perpendicularly in the experimental arrangement.

Results and discussion

The optical (Fig. 1(e,f) and corresponding confocal fluorescence images (Fig.1(g,h)) respectively of ZnO:Er^{3+} and ZnO:Er^{3+}: Ag NPs integrated under UV (375nm) excitation clearly show regions of bright fluorescence as well as greater emission intensity from ZnO:Er^{3+} in proximity with Ag NPs (Fig.1h). The corresponding integrated emission spectra (Fig. 1i) of ZnO:Er^{3+} in propinquity with Ag NPs (predominantly hexagonal Ag NPs~50nm) clearly elucidates enhancements in fluorescence upto 546% (at 442nm) as compared to ZnO:Er^{3+} under UV excitation. The significant fluorescence enhancement

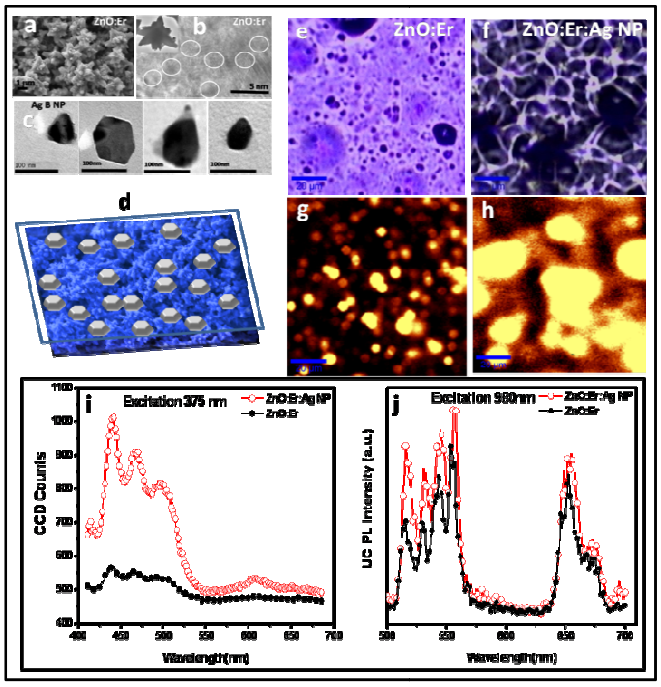

Fig.1 (colour online) SEM image of flower like ZnO:Er^{3+} (a); HRTEM image showing lattice fringes of individual nanoparticles of ZnO:Er^{3+} (b), inset shows the TEM image of single nanoflower; collage of TEM images of Ag NPs (c); graphical representation (not to scale) (d) of integrated ZnO:Er^{3+} (blue flowers, exact SEM image), PVA layer (blue transparent layer) Ag NPs (metallic silver hexagons) hybrid structure used for confocal fluorescence study. Optical image and corresponding confocal fluorescence image of (e) & (g) ZnO:Er^{3+}; (f) & (h) ZnO:Er^{3+}-Ag NP hybrid under 375nm UV excitation; corresponding confocal fluorescence (integrated) spectra under 375nm laser excitation (i) and UC PL spectra of the ZnO:Er^{3+} (black curve) and ZnO:Er^{3+}-Ag NP hybrid structure (red curve) under 980nm laser excitation (j).

could be attributed to the plasmonic coupling of EM field of the Ag NPs with bound excitons of the ZnO nanoparticles[20].

The measured upconversion photoluminescence (PL) emission spectra of the hybrid nanostructure of ZnO:Er^{3+} with Ag NPs under 980 nm laser excitation is shown in Fig.1(j) which shows both green and red UC emission. The spectrum reveals enhancement in the emission intensity when ZnO:Er^{3+} nanoparticles are conjugated with Ag NPs in the hybrid system. The UC fluorescence enhancement due to plasmonic effect is 174.5% for 516nm peak, 152.8% for 531nm peak, 132.6% for 545nm peak and 115.7% for 655nm red peak as compared to ZnO:Er^{3+} under IR excitation. As the emission wavelength increases, there can be partial absorption of the emitted fluorescence by Ag NPs as emitted fluorescence can activate Ag NPs as their absorption becomes strong in that spectral region (Fig.2c). Hence enhancement is lower at 655nm emission wavelength.

Ag nanowire enhanced upconversion emission has been reported for $NaYF_4$:Yb^{3+},Er^{3+} system[21] and $NaYF_4$:Yb^{3+}/Tm^{3+} coated with Au nanoparticles[22] but no such report is available for UC enhancement in RE dope ZnO. This study clearly indicates that the upconversion emission in ZnO can be enhanced by SPR tuned Ag NPs. The Ag NPs localize the incident EM field in different plasmonic modes as near field around them contributing towards the fluorescent enhancements. The measured UV-visible absorption spectrum of Ag NP colloidal solution (Fig 2c) exhibits a quadrupolar resonance peak at 335nm which covers the excitation range of ZnO:Er^{3+} (supporting information Fig. S3). The broad dipolar peak centered at 795 nm extends well up to 1000 nm in the absorption spectra. The well matched spectral overlap of the excitation range of upconversion nanoparticles as revealed in the measured absorption spectra of the Ag NPs in the near IR region (Fig.2c), clearly suggests the enhancements of excitation leading to UC fluorescence enhancement.

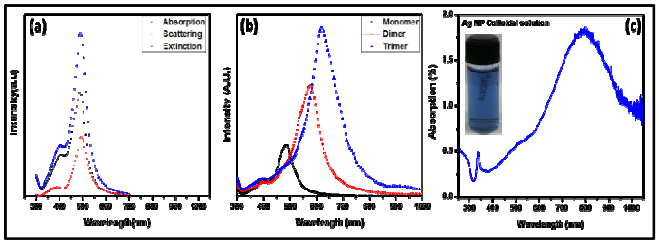

Fig 2 (colour online) FDTD simulated absorption, scattering and extinction spectra of Ag nanohexagon (a) and the shift in extinction spectra from monomer to dimer to trimer (b), experimental UV-Visible absorption spectra of Ag NP colloidal solution, inset shows actual photographs of colloidal solution.

To elucidate the influence of near field generated around Ag NPs of different shape, as used in the experiment, in inducing fluorescence enhancements, the three dimensional finite difference time domain (FDTD) simulations of the exact Ag NP and their hybrids were carried out. One Ag NP from the solution was considered for the simulation on the basis of the average geometrical distribution. The representative Ag NP chosen is nanohexagon and the image was imported from transmission electron micrograph for FDTD simulation. The FDTD technique is well proven to solve Maxwell's electromagnetic equation for plasmonic structures with complex geometries that considers both the E(t) and H(t) components discrete over time[23]. The steady-state continuous wave field E(ω) is then calculated by Fourier transformation of E(t) during simulations. All the simulations were performed with light injected along Z-axis which is perpendicular to the thin film, thus conforming to the experimental set up. FDTD solutions (version 8.7.1)[24] was employed to perform the simulations with mesh size 0.8nm so that results with higher degree of accuracy could be obtained. The material response was taken from Palik[25] (0-2μm) and the field was allowed to evolve for 200fs. FDTD method was employed to calculate the absorption, scattering and extinction, spectra for the Ag nanohexagon (Fig.2a). In the experimental set up, number of Ag NPs and their aggregates are deposited on the ZnO:Er^{3+} NPs. To estimate such effects of plasmonic coupling between closely spaced Ag NPs, particle hybrids such as dimers and trimers in a linear arrangement with inter particle separation of 5nm were simulated through FDTD. The extinction spectra for nanohexagon dimer and trimer (~50nm, separated by 5nm) were also calculated to see the effect of particle hybrids and are shown in Fig 2(b). As the particle size of the hexagonal Ag NP is about 50nm, non radiative damping due to electron phonon interaction resulting in absorption as well as radiative resonant scattering of Plasmon modes is operative[26]. For a single nanohexagon, the extinction peak is at 488nm which red shifts to 576nm for dimer and 616nm for trimer. It is also known from FDTD simulation that as number of particles in a particle hybrid system increases, the extinction spectrum broadens and red shifts[26,27] due to interaction of plasmonic modes of neighbouring Ag NPs[12]. Moreover, formation of clusters or closely spaced nanoparticle hybrids in the film leads to coupling of plasmon modes and enhancement of local EM field [11,12]. In near field coupling between Ag NPs, the restoring force operative upon oscillating electron cloud of individual NP could increase or decrease by the charge distribution of proximate particles. In a longitudinal array of Ag NPs, red shifts of SPR of longitudinal modes can happen[28]. The absorption spectrum of Ag NP colloidal solution as measured by UV-visible spectroscopy (Fig 2(c)) represent absorption profile of a random distribution of Ag NPs in a homogenized medium. The observed broad absorption peak can be attributed to the inhomogeneous damping caused by different spatial positions and random orientations of Ag NPs in colloidal solution giving rise to different peak positions and the broad curve can be understood as convolution of all resulting peaks together (see supporting information S4)[11].

For a quantitative comparison of the effect of Ag NPs on the rare earth doped ZnO particles, FDTD method was employed to calculate the generated EM field for the hexagonal Ag NP geometry at excitation wavelengths 375nm, 980nm and also at localized surface Plasmon resonance (LSPR) frequency. Near field images of simulated EM field ($|E|$) of Ag nanohexagon (Fig.3a-c) and dimers (Fig.3d-f) at 375nm, 795nm (LSPR) and 980nm respectively, undoubtedly shows the hotspots due to diploar, quadrupolar modes and lightening rod effect.

The local electric field values $|E|^2$ listed in Table1 obviously reveals largest $|E|^2$ values at the dipolar LSPR frequency. At 375nm excitation wavelength the calculated $|E|^2$ value for the Ag

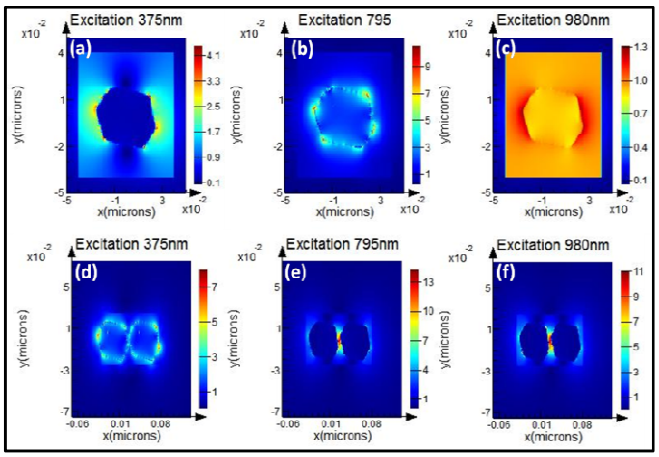

Fig.3 (colour online) Near field ($|E|$) images at different incident wavelengths by FDTD simulation of exact Ag nanohexagon and dimers.

nanohexagon is 19 times that of the incident field. However when 980nm wavelength is incident on the Ag NPs, the $|E|^2$ value is calculated to be 11 times for Ag NP[12]. The simulated near field images of the exact Ag NP thus clearly elucidate the confined near field under different excitation wavelengths. The field enhancement increases manifold for dimer e.g., 295 times, 63 times and 22 times that of incident EM field at SPR, 375nm and 980nm respectively. The field enhancement for dimer is 2-3 times that of monomer at incident optical field of different incident frequencies (table1). Such E-field enhancements occur due to confinement of field in the intergap region of Ag NPs as well as around them as is clearly elucidated in Fig.3(d-f)[29]. Larger enhancements are expected for larger ensembles of particles. Such collection of dimers of Ag NPs have also been used to explain metal enhanced fluorescence in ZnMgO[30].

The near field enhancements of Ag NP and their hybrids at UV and IR excitation wavelengths are thus commensurate with the observed fluorescence enhancement at these respective excitation wavelengths corresponding to down and up conversion emission from ZnO:Er^{3+} (Fig.1 i & j). The generated strong near field by Ag NPs enhances the total electric field experienced by Er^{3+} ions and as the radiative transitions of Er^{3+} ions is electric dipole in origin, non linear optical process leading to upconversion emission is enhanced. The coupling of Er^{3+} excited state and Ag NP dipolar LSPR modifies the Stark shift[29]. As a result of change in local electric field adjacent to RE ion due to coupling with Ag NP, the emission peaks are red shifted (Fig.1j) by few nm with an appreciable increase in luminescence. The $|E|^2$ values obtained from FDTD solutions of Ag NP monomer and dimer under 980nm incident field clearly reveals the correlation of generated near field and UC luminescence enhancement.

It is well known that metal enhanced fluorescence can occur either through excitation enhancement (enhancement of local EM field) and/or through emission enhancement (enhancement of radiative decay rate). However it is difficult to distinguish between the contributions of these two components, particularly when broad SPR band of Ag NPs (Fig.2c) overlap with both excitation and emission spectrum of the ZnO:Er^{3+} nanoparticles. Excitation enhancement produces a higher excitation rate but does not change

Table 1: Near field enhancement of Ag nanohexagon.

E-Field Enhancement $\|E\|^2$ (Z-direction)			
Ag NP	SPR	375nm	980nm
Monomer	112	19	11
Dimer	295	63	22

the lifetime of the fluorophore. On the other hand, emission enhancement increases the radiative decay rate thus reducing the luminescence decay time[31]. In our case, when Ag NPs are conjugated with ZnO:Er^{3+} nanoparticles, we have measured the luminescence decay under 375 nm excitation as shown in Fig.4 and observed that decay characteristics remain almost similar with and without Ag NPs. This suggests that prominent mechanism for visible fluorescence enhancement in ZnO:Er^{3+} would be through enhancemet of near field due to presence of Ag NPs in proximity through excitation enhancement. If scattering of metal nanoparticles are responsible for such fluorescence enhancement, then scattering spectra must reflect such spectral dependence. The FDTD calculated scattering spectra (Fig.2a) show a maxima around 500nm and negligible scattering at 442nm where we observed 546% enhancement. Moreover, it is well known that scattering contributes to emission enhancement when SPR band overlaps with emission spectra of the fluorophore and confirmation of such effect comes from luminescence decay measurement where emission enhancement increases the radiative decay rate thus reducing the luminescence decay time. But our experimental results of decay measurements (Fig.4) conclusively prove that there is no change in decay time and the fluorescence enhancement is not through scattering but due to higher excitation rate (excitation enhancement) due to increase in plasmonic near field.

Thus tuning of plasmonic modes in the UV–IR region of EM spectra through shape tailoring of Ag NPs can lead to coupling of specific modes with excitation frequency of the ZnO:Er^{3+} nanoparticles and lead to fluorescence enhancement under both UV and IR excitation. Strong enhancement in fluorescence emission from ZnMgO has been reported due to coupling interaction between the hybridized quadrupole plasmon in Ag nanoparticle aggregates which were recognized as collection of dimers[30]. It was also shown by theoretical simulation that overlapping of the radiative quadrupolar mode with the emission band of excited fluorophores assist fluorescence emission due to an enhancement in the quantum efficiency[32]. Higher-order plasmonic multipolar modes were shown to couple with the incident EM field[33-36], opening up possibilities to harness the higher order mode as well as dipolar mode for fluorescence augmentation concurrently through excitation and emission processes. Thus, in our case, tuning of quadrupole resonance in short wavelength region and dipole resonance in long

wavelength region of Ag nanohexagons are responsible for fluorescence enhancement under UV and IR excitation respectively.

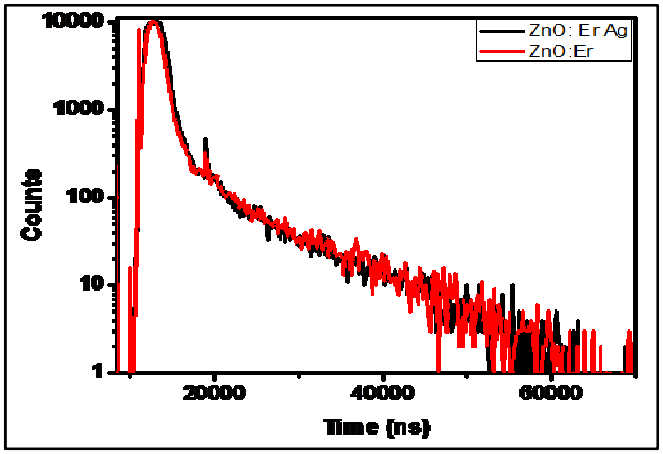

Fig.4 Luminescence decay curve of blue emission under 375nm excitation.

The dual mode energy transfer scheme from Ag NPs to Er^{3+} doped ZnO nanoparticles is indicated in the energy level diagram (Fig.5). For down conversion, the energy level diagram illustrates cohesive energy transfer (ET) from Ag NP corresponding to quadrupolar oscillations (QD) together with the direct excitations of the ZnO nanoparticles under UV pump giving rise to emission peaks in the blue - green spectral region (Fig.5).The visible emission is a consequence of radiative recombination of electrons hole pairs in the intrinsic donor acceptor pair defect states. For up conversion emission in ZnO: Er^{3+}, absorption of a 980nm photon by Er^{3+} ions in the ground state ($^4I_{15/2}$) elevates it to excited $^4I_{11/2}$ state which again can resonantly absorb another IR photon to go to $^4F_{7/2}$ state. Subsequent radiative transition to ground state or phonon assisted relaxation to lower excited states followed by radiative transition to ground state result in green and red UC emission as depicted in the energy level diagram (Fig. 5). Effective ET can happen from Ag NP corresponding to dipolar plasmonic mode (ED) to Er^{3+} leading to enhancement of fluorescence.

Conclusions

In summary, we present a comprehensive work involving chemical synthesis of shape tailored silver nanoparticles for effective tuning of surface Plasmon modes and near field generated around them, chemical synthesis of flower shaped Er^{3+} doped ZnO nanoparticles, conjugation of Ag NP - ZnO:Er^{3+} hybrid nanostrucrure in an appropriate configuration that lead to fluorescence enhancement in dual excitation (UV and IR) mode. We have provided conclusive proof that fluorescence enhancement do occur due to plasmonic effect of Ag NPs in proximity of emitting ZnO:Er^{3+} nanoparticles with both experimental results and theoretical simulation. Conclusive evidence of coupling of different plasmonic mode of Ag NPs (nanohexagon) causing enhancement of fluorescence has been unequivocally established through confocal fluorescence mapping & spectroscopy of

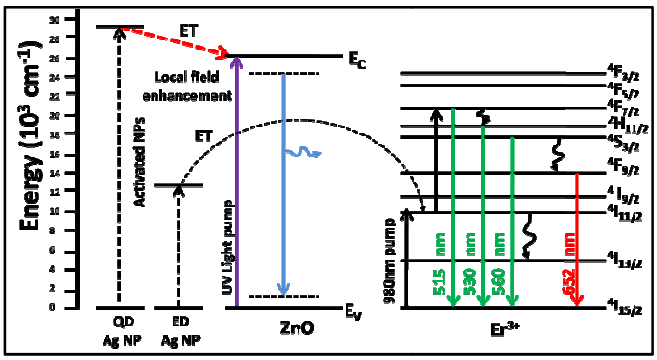

Fig.5 (colour online) Energy level diagram showing excitation of Ag NP and energy transfer (ET) corresponding to quadrapolar resonance (QD) to ZnO under UV pump and also the ET corresponding to dipolar resonance (ED) from Ag NP to Er^{3+} level under 980nm pump laser, the emission transitions are indicated by downward arrows.

ZnO:Er^{3+} and ZnO:Er^{3+} - Ag NP integrated system along with UV-visible absorption spectroscopy of Ag NPs that exhibit a quadrupolar peak in the UV region and the broad dipolar peak covering the near IR region encompassing the excitation range of ZnO:Er^{3+}. For a comprehensive understanding of the experimental results, we have used the most suitable and sophisticated simulation technique FDTD for estimating the near field generated by Ag NPs and their hybrids under UV and IR excitation wavelengths which showed that field enhancements are manifold compared to the incident field (table1) and also their extinction properties. As the enhancement of local EM field contributes to excitation enhancement, fluorescence enhancement occurs. This is also proven by luminescence decay measurement where decay characteristics do not change which is a signature of excitation enhancement through enhancement of plasmonic near field. A comprehensive correlation of the degree of fluorescence enhancement with the near field generated has been established through FDTD simulation of Ag nanohexagon and their dimmers at different incident wavelengths. Such dual mode enhancement of fluorescence through plasmonic mode coupling of shape tailored Ag NPs has not been reported so far. Plasmon mediated fluorescence enhancements in metal-semiconductor ensembles offer new scope in better solar energy harvesting, nanobiotechnology, lighting industry.

Acknowledgements

The authors are grateful to CSIR TAPSUN programme for funding and Mithun Bhomkar for help in FDTD simulation.

Notes and references

Luminescent Materials Group, CSIR-National Physical Laboratory, Dr.K.S.Krishnan Road, New Delhi-110012, India

Corresponding Author

*E-mail santa@nplindia.org

† *Sample synthesis*

Trivalent rare earth Er^{3+} (2 atomic%) doped ZnO nanoparticles were synthesized by co-precipitation (CPP) method at room temperature using submolar precursor solutions of zinc acetate and erbium nitrate in alkaline environment (pH 10). The silver nanoparticles were synthesized using

optimal concentrated solutions of $AgNO_3$, PVP and Tri-sodium citrate. The desired shape and size of the nanoparticles were tailored using optimized concentrations of $NaBH_4$ as well as H_2O_2 (30% w/v).

UV-Visible absorption measurements

The absorption spectra of the Ag NP solution were measured by Avantes UV-Visible spectrometer.

Thickness measurement

The thickness of PVA flim was measured with Stylus Profilometer (Ambios XP200)

Fluorescence measurements

Confocal fluorescence microscopy (WITec alpha 300M+) was employed to study the hybrid thin film material system with 100X microscope objective (N.A 0.9) and UV diode laser (output λ~375nm, power 10mW, Toptica) as exciting source. The up conversion photo luminescence measurements in ZnO:Er^{3+} and Ag NP conjugated samples were done by using a power tunable 980 nm diode laser (MDL-N-980-6W) coupled with optical fiber, as excitation source and Edinburgh Instruments fluorescence spectrometer (FLSP920). Time resolved photoluminescence (PL) decay was measured using Edinburgh Instruments Time resolved Spectrometer (FLSP920] using a pulsed Xe lamp as excitation source and employing time correlated single photon counting (TCSPC) technique

FDTD simulation

The calculation of near field and extinction properties of silver nanohexagon was done by FDTD method (Lumerical FDTD solutions 8.5). The refractive index of the surrounding medium was kept 1.33. We used Conformal Variant 1 mesh refinement option and standard PML boundaries were used to prevent reflections from absorbing boundaries. We used a broadband total field scattering field (TFSF) source and implemented suitable monitors to calculate the near field and extinction properties of silver nanohexagons. A plane wave source as the incident optical field was injected from Z- axis falling perpendicularly on silver nanohexagons resting on a plane and this configuration exactly conforms to the setup used for confocal fluorescence measurements

.

Electronic Supplementary Information (ESI) available:

Figure S1 XRD spectra of ZnO:Er^{3+}

Figure S2 SEM, TEM of ZnO:Er^{3+} and TEM of Ag NPs

Figure S3 PL excitation spectra of ZnO:Er^3

Figure S4 FDTD simulated absorption and scattering spectra of Ag NPs by injecting incident light from X, Y direction. The real and imaginary part of dielectric function of Ag NP (from Palik's model) and the corresponding FDTD model fit.

1. M Achermann, J.Phys.Chem.Lett.1, 2837 (2010).
2. C.D Geddes, Metal enhanced fluorescence, (John Wiley & SonsNew Jersey 2010), P 91
3. C.W.Lai, J.An and H.C. Ong, Appl.Phys.lett. **86**, 251105 (2005).
4. W.H.Ni, J.An, C.W.Lai, H.C.Ong and J.B.Xu, J Appl Phys **100**, 026103 (2006).
5. P.H.Cheng, D.S.Li, Z.Z.Yuan and D.R.Yang, Appl. Phys Lett **92**, 041119(2008).
6. H.Lu, X.Xu,L.Lu, M.Gong and Yansong Liu, J Phys:Condens.Matter **20**, 472202 (2008).
7. J.B.You, X.W.Zhang, Y.M.fan, S.Qu and N.F.Chen, Appl.Phys Lett. **91**, 231907 (2007).
8. X. H. Xiao F. Ren X. D. Zhou,T. C. Peng, W. Wu,X. N. Peng, X. F. Yu,and C. Z. Jiang, Appl Phys Lett. **97**, 071909 (2010).
9. M. E.Aguirre, H. B. Rodríguez, E.S. Roman, A. Feldhoff, and M.A. Grela,, J. Phys. Chem. C **115**, 24967 (2011).
10. Q.Wang, F. Song et al., Opt. Express, **19** (8), 6999 (2011).
11. Z. Buch, V.Kumar, H. Mamgain, S.Chawla, Chem Com **49**, 9845 (2013).
12. Z. Buch, V.Kumar, H. Mamgain, S.Chawla,J Phys Chem Lett **4**, 3834 (2013).
13. W. Feng et al.Chem Comm. (2009),4393
14. F. Zhang et al. JACS (2010)132,2850.
15. S. Schietinger et al., Nano Lett. (2010)10,134
16. Y. Wu et al., J. Phys. Chem. (2011) 115, 25040
17. G.S. Meutrax and C.A.Mirkin, Adv.Matter 17 (4), 412 (2005).
18. P. Anger; P. Bharadwaj; L. Novotny; Phys.Rev.Lett., 96,113002 (2006).
19. F.K.Guedje, M.Giloan, M.Potara, M.N.Hounkonnou and S. Astilean , Phys Scr. **86**, 055702 (2012).
20. S.A.Maier, P.G. Kik and H.A.Atwater, Appl.Phys.Lett. **81**, 9(2002).
21. W.Feng, L.D.Sun, and C.H.Yan, ChemComm .4393-4395(2009).
22. H. Z. Li, I. A. Ivanov, Y. Qu,Y.u Huang and X. Duan, Angew.Chem, 2865-2868 (2010).
23. A. Taflove, S.C Hagness, Computational Electrodynamics: The Finite-Difference Time Domain Method. Artech House (2000).
24. Reference Guide for FDTD Solutions, www.lumerical.com/fdtd,(2013)
25. E.D. Palik, Handbook of optical constants of solids, Academic Press,New York(1985).
26. D.D.Evanoff Jr and G.Chumanov, ChemPhysChem **6**, 1221(2005).
27. S.A.Maier, "Plasmonics:Fundamentals and Applications", Springer New York, 8 (2004),80.11.
28. V.A.G.Rivera,F.A.Ferri and E.Marega Jr. Plasmonics-Principles and Applications, 283-312, Intech (2012).
29. Xu, H.; Bjerneld, E. J.; Kall, M.; Borjesson, L.Phys. Rev. Lett. 1999, **83**, 4357–4360.
30. H.Y. Chen, K.W. Liu, M.M. Jiang, Z.Z. Zhang, X.H. Xie, D.K. Wang, L. Liu, B.H. Li, D.X. Zhao, C.X. Shan, and D.Z. Shen, Appl. Phys. Lett. 104, 091119 (2014).
31. W.Deng,L Sudheendra, JK.Zhao, J.Fu, D.Jin,I M Kennedy and E M Goldys, Nanotechnology,22,325604(2011).

32. T. Zhang, G. Lu, J. Liu, H. Shen, P. Perriat, M. Martini, O. Tillement, Q. Gong, Appl. Phys. Lett. 101, 051109 (2012)

33. F. Hao, E. M. Larsson, T. A. Ali, D. S. Sutherland, and P. Nordlander, Chem. Phys. Lett. 458, 262 (2008).

34. H. Wang, Y. Wu, B. Lassiter, C. L. Nehl, J. H. Hafner, P. Nordlander, and N. J. Halas, Proc. Natl. Acad. Sci. U.S.A. 103, 10856 (2006)

35. F. Hao, P. Nordlander, Y. Sonnefraud, P. V. Dorpe, and S. A. Maier, ACS Nano 3, 643 (2009); Z. Yang, Z. Zhang, L. Zhang, Q. Li, Z. Hao, and Q. Wang, Opt. Lett. 36, 1542 (2011)

36. S. Zhang, K. Bao, N. J. Halas, H. Xu, and P. Nordlander, Nano Lett. 11, 1657 (2011)

.